The Astrophysical Journal, 640:1051–1062, 2006 April 1

HOW DRY IS THE BROWN DWARF DESERT? QUANTIFYING THE RELATIVE NUMBER OF PLANETS, BROWN DWARFS, AND STELLAR COMPANIONS AROUND NEARBY SUN-LIKE STARS

Daniel Grether[1] and Charles H. Lineweaver[1,2]
Received 2004 December 14; accepted 2005 November 29

ABSTRACT

Sun-like stars have stellar, brown dwarf, and planetary companions. To help constrain their formation and migration scenarios, we analyze the close companions (orbital period <5 yr) of nearby Sun-like stars. By using the same sample to extract the relative numbers of stellar, brown dwarf, and planetary companions, we verify the existence of a very dry brown dwarf desert and describe it quantitatively. With decreasing mass, the companion mass function drops by almost 2 orders of magnitude from 1 $M_\odot$ stellar companions to the brown dwarf desert and then rises by more than an order of magnitude from brown dwarfs to Jupiter-mass planets. The slopes of the planetary and stellar companion mass functions are of opposite sign and are incompatible at the 3 σ level, thus yielding a brown dwarf desert. The minimum number of companions per unit interval in log mass (the driest part of the desert) is at $M = 31^{+25}_{-18} M_J$. Approximately 16% of Sun-like stars have close ($P < 5$ yr) companions more massive than Jupiter: $11\% \pm 3\%$ are stellar, $<1\%$ are brown dwarf, and $5\% \pm 2\%$ are giant planets. The steep decline in the number of companions in the brown dwarf regime, compared to the initial mass function of individual stars and free-floating brown dwarfs, suggests either a different spectrum of gravitational fragmentation in the formation environment or post-formation migratory processes disinclined to leave brown dwarfs in close orbits.

Subject headings: stars: low-mass, brown dwarfs

Online material: machine-readable table

1. INTRODUCTION

The formation of a binary star via molecular cloud fragmentation and collapse, and the formation of a massive planet via accretion around a core in a protoplanetary disk, both involve the production of a binary system but are usually recognized as distinct processes (e.g., Heacox 1999; Kroupa & Bouvier 2003; see, however, Boss 2002). The formation of companion brown dwarfs, with masses in between the stellar and planetary mass ranges, may have elements of both or some new mechanism (Bate 2000; Rice et al. 2003; Jiang et al. 2004). For the purposes of our analysis brown dwarfs can be conveniently defined as bodies massive enough to burn deuterium ($M \gtrsim 13 M_J$) but not massive enough to burn hydrogen ($M \lesssim 80 M_J$; e.g., Burrows et al. 1997). Since fusion does not turn on in gravitationally collapsing fragments of a molecular cloud until the final masses of the fragments are largely in place, gravitational collapse, fragmentation, and accretion should produce a spectrum of masses that does not know about these deuterium and hydrogen burning boundaries. Thus, these mass boundaries should not necessarily correspond to transitions in the mode of formation. The physics of gravitational collapse, fragmentation, accretion disk stability, and transfer of angular momentum should be responsible for the relative abundances of objects of different masses, not fusion onset limits.

However, there seems to be a brown dwarf desert—a deficit in the frequency of brown dwarf companions relative to the frequency of either less massive planetary companions (Marcy & Butler 2000) or more massive stellar companions to Sun-like hosts. The goal of this work is to (1) verify that this desert is not a selection effect due to our inablility to detect brown dwarfs and (2) quantify the brown dwarf desert more carefully with respect to both stars and planets. By selecting a single sample of nearby stars as potential hosts for all types of companions, we can better control selection effects and more accurately determine the relative number of companions more and less massive than brown dwarfs.

Various models have been suggested for the formation of companion stars, brown dwarfs, and planets (e.g., Larson 2003; Kroupa & Bouvier 2003; Bate 2000; Matzner & Levin 2005; Boss 2002; Rice et al. 2003). All models involve gravitational collapse and a mechanism for the transfer of energy and angular momentum away from the collapsing material.

Observations of giant planets in close orbits have challenged the conventional view in which giant planets form beyond the ice zone and stay there (e.g., Udry et al. 2003). Various types of migration have been proposed to meet this challenge. The most important factors in determining the result of the migration is the time of formation and mass of the secondary and its relation to the mass and time evolution of the disk (e.g., Armitage & Bonnell 2002). We may be able to constrain the above models by quantitative analysis of the brown dwarf desert. For example, if two distinct processes are responsible for the formation of stellar and planetary secondaries, we would expect well-defined slopes of the mass function in these mass ranges to meet in a sharp brown dwarf valley.

We examine the mass and period distributions for companion brown dwarfs and compare them with those of companion stars and planets. The work most similar to our analysis has been carried out by Heacox (1999), Zucker & Mazeh (2001b), and Mazeh et al. (2003). Heacox (1999) and Zucker & Mazeh (2001b) both combined the stellar sample of Duquennoy & Mayor (1991) along with the known substellar companions and identified different mass functions for the planetary mass regime below $10 M_J$ but found similar flat distributions in logarithmic mass for brown dwarf and stellar companions. Heacox (1999) found that the logarithmic mass

[1] Department of Astrophysics, School of Physics, University of New South Wales, Sydney, NSW 2052, Australia.
[2] Planetary Science Institute, Research School of Astronomy and Astrophysics and Research School of Earth Sciences, Australian National University, Canberra, ACT, Australia.

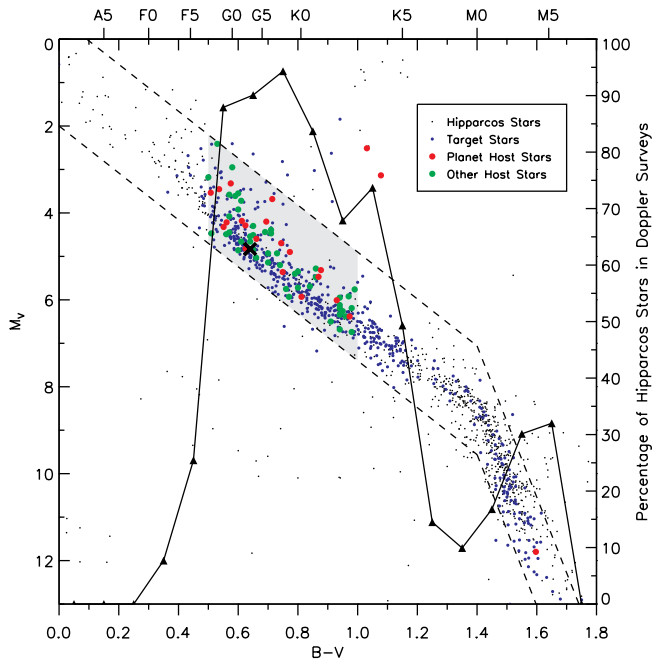

FIG. 1.—Our close sample. Hertzsprung-Russell diagram for *Hipparcos* stars closer than 25 pc. Small black dots are *Hipparcos* stars not being monitored for possible companions by one of the eight high-precision Doppler surveys considered here (Lineweaver & Grether 2003). Larger blue dots are the subset of *Hipparcos* stars that are being monitored ("target stars") but have as yet no known planetary companions. The still larger red dots are the subset of target stars hosting detected planets ("planet host stars"), and the green dots are those hosts with larger mass ($M_2 > 13M_J$) companions ("other host stars"). Only companions in our less biased sample ($P < 5$ yr and $M_2 > 10^{-3}\ M_\odot$) are shown (see § 2.2). Our Sun is shown as the black cross. The gray parallelogram is the region of M_V-$(B-V)$ space that contains the highest fraction (*triangles*) of *Hipparcos* stars that are being monitored for exoplanets. This Sun-like region—late F to early K type main-sequence stars—contains our *Hipparcos* Sun-like Stars. The target fraction needs to be as high as possible to minimize selection effects potentially associated with companion frequency. The target fraction is calculated from the number of main-sequence stars, i.e., the number of stars in each bin between the two dashed lines. This plot contains 1509 *Hipparcos* stars, of which 627 are Doppler target stars. The Sun-like region contains 464 *Hipparcos* stars, of which 384 are target stars. Thus, the target fraction in the Sun-like gray parallelogram is ~83% (=384/464).

function in the planetary regime is best fit by a power law with a slightly negative slope, whereas Zucker & Mazeh (2001b) found an approximately flat distribution. Mazeh et al. (2003) looked at a sample of main-sequence stars using infrared spectroscopy and combined them with the known substellar companions and found that in log mass, the stellar companions reduce in number toward the brown dwarf mass range. They identify a flat distribution for planetary mass companions. We discuss the comparison of our results to these in § 3.1.

2. DEFINING A LESS BIASED SAMPLE OF COMPANIONS

2.1. *Host Sample Selection Effects*

High-precision Doppler surveys are monitoring Sun-like stars for planetary companions and are necessarily sensitive enough to detect brown dwarfs and stellar companions within the same range of orbital period. However, to compare the relative abundances of stellar, brown dwarf, and planetary companions, we cannot select our potential hosts from a non-overlapping union of the FGK spectral type target stars of the longest running, high-precision Doppler surveys that are being monitored for planets

TABLE 1
SUN-LIKE 25 pc SAMPLE

Hipparcos Number	$B-V$	M_V	Distance (pc)	Exoplanet Target	Companion ($P < 5$ yr) ($M > M_J$)
HIP 171.....	0.69	5.33	12.40	Yes	
HIP 518.....	0.69	4.44	20.28	No	Star
HIP 544.....	0.75	5.39	13.70	Yes	
HIP 1031.....	0.78	5.68	20.33	Yes	
HIP 1292.....	0.75	5.36	17.62	Yes	Planet

NOTES.—Table 1 is published in its entirety in the electronic edition of the *Astrophysical Journal*. A portion is shown here for guidance regarding its form and content.

(Lineweaver & Grether 2003). This is because Doppler survey target selection criteria often exclude close binaries (separation $<2''$) from the target lists and are not focused on detecting stellar companions. Some stars have also been left off the target lists because of high stellar chromospheric activity (Fischer et al. 1999). These surveys are biased against finding stellar mass companions. We correct for this bias by identifying the excluded targets and then including in our sample any stellar companions from other Doppler searches found in the literature. Our sample selection is illustrated in Figure 1 and detailed in Table 1 (complete list in the electronic version only) for stars closer than 25 pc and Figure 2 for stars closer than 50 pc.

Most Doppler survey target stars come from the *Hipparcos* catalog (ESA 1997) because host stars need to be both bright and have accurate masses for the Doppler method to be useful in determining the companion's mass. One could imagine that the

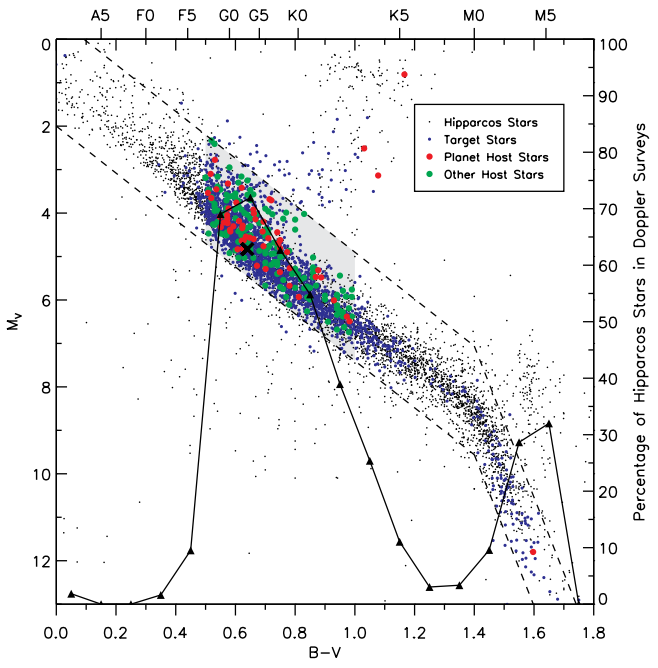

FIG. 2.—Our far sample. Same as Fig. 1, but for all *Hipparcos* stars closer than 50 pc. The major reason the target fraction (~61%, *triangles*) is lower than in the 25 pc sample (~83%) is that K stars become too faint to include in many of the high-precision Doppler surveys where the apparent magnitude is limited to $V < 7.5$ (Lineweaver & Grether 2003). This plot contains 6924 *Hipparcos* stars, of which 2351 are target stars. The gray parallelogram contains 3296 *Hipparcos* stars, of which 2001 are high-precision Doppler target stars (61% ~ 2001/3296). The stars below the main sequence and the stars to the right of the M dwarfs are largely due to uncertainties in the *Hipparcos* parallax or $B-V$ determinations.

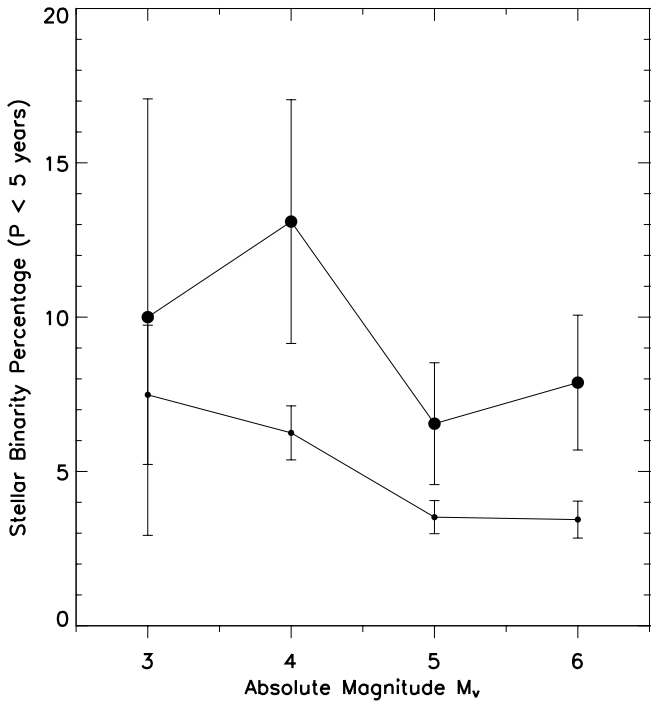

FIG. 3.—Fraction of stars that are known to be close ($P < 5$ yr) Doppler binaries as a function of absolute magnitude. For the 25 pc Sun-like sample (*large dots*), ~11% of stars are binaries; within the error bars, brighter stars do not appear to be significantly overrepresented. If we include the extra stars to make the 50 pc Sun-like sample (*small dots*), the stellar binary fraction is lower and decreases as the systems get fainter.

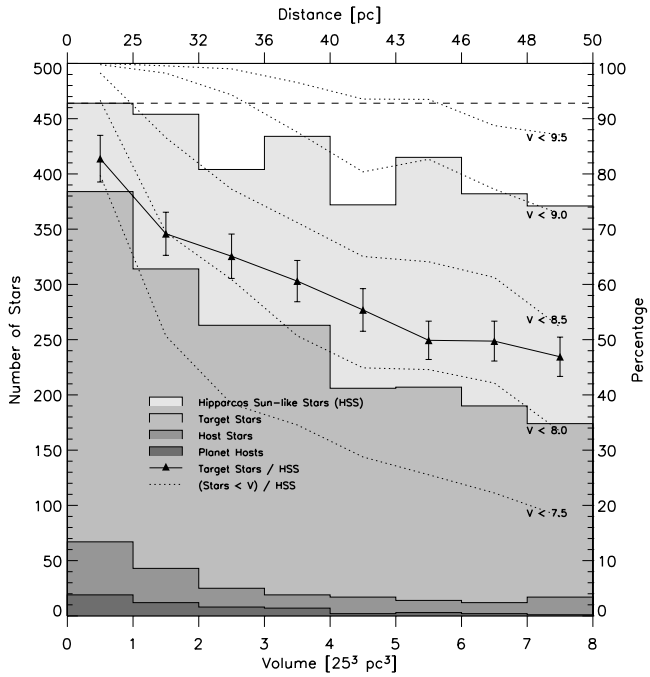

FIG. 4.—Distance dependence of sample and companions. Here we show the number of nearby Sun-like stars as a function of distance. Each histogram bin represents the stars in an equal-volume spherical shell. Hence, a sample that is complete in distance out to 50 pc would produce a flat histogram (*horizontal dashed line*). The lightest shade of gray represents *Hipparcos* Sun-like Stars out to 50 pc that fall within the parallelogram of Fig. 2 ("HSS"). The next darker shade of gray represents *Hipparcos* stars that are being monitored for planets using the high-precision Doppler techniques (eight groups described in Lineweaver & Grether 2003). The triangles represent this number as a fraction of *Hipparcos* stars. This fraction needs to be as large as possible to minimize distance-dependent selection effects in the target sample potentially associated with companion frequency. Also shown (*darker gray*) are the number of *Hipparcos* stars that have one or more companions in the mass range $10^{-3} < M/M_{\odot} < 1$ and those that host planets (*darkest gray*). Only those companions in the less biased sample, $P < 5$ yr and $M_2 > 10^{-3}\ M_{\odot}$, are shown (§ 2.2). The fraction of stars having an apparent V magnitude brighter (lower) than a given value are shown by the five dotted lines for $V < 7.5$–9.5.

Hipparcos catalog would be biased in favor of binarity since hosts with bright close-orbiting stellar companions would be overrepresented. We have checked for this overrepresentation by looking at the absolute magnitude dependence of the frequency of stellar binarity for systems closer than 25 and 50 pc (Fig. 3). We found no significant decrease in the fraction of binaries in the dimmer stellar systems for the 25 pc sample and only a small decrease in the 50 pc sample. Thus, the *Hipparcos* catalog provides a good sample of potential hosts for our analysis, since (1) it contains the Doppler target lists as subsets, (2) it is volume-limited for Sun-like stars out to ~25 pc (Reid 2002), and (3) it allows us to identify and correct for stars and stellar systems that were excluded. We limit our selection to Sun-like stars ($0.5 \leq B - V \leq 1.0$) or approximately those with a spectral type between F7 and K3. Following S. Udry (2004, private communication) and the construction of the Coralie target list, we limit our analysis to main-sequence stars, or those between −0.5 and +2.0 dex (below and above), an average main-sequence value as defined by $5.4(B - V) + 2.0 \leq M_V \leq 5.4(B - V) - 0.5$. This sampled region, which we call our "Sun-like" region of the H-R diagram, is shown by the gray parallelograms in Figures 1 and 2.

The *Hipparcos* sample is essentially complete to an absolute visual magnitude of $M_V = 8.5$ (Reid 2002) within 25 pc of the Sun. Thus, the stars in our 25 pc Sun-like sample represent a complete, volume-limited sample. In our sample we make corrections in companion frequency for stars that are not being targeted by Doppler surveys as well as corrections for mass and period companion detection selection effects (see § 2.2). The result of these corrections is our less biased distribution of companions to Sun-like stars within 25 pc. We also analyze a much larger sample of stars out to 50 pc to understand the effect of distance on target selection and companion detection. Although less complete, with respect to the relative number of companions of different masses, the results from the 50 pc sample are similar to the results from the 25 pc sample (§ 3).

Stars in our Sun-like region are plotted as a function of distance in Figure 4. Each histogram bin represents an equal volume spherical shell; hence, a sample complete in distance would produce a flat histogram. Also shown are the target stars, which are the subset of *Hipparcos* stars that are being monitored for planets by one of the eight high-precision Doppler surveys (Lineweaver & Grether 2003) analyzed here. The triangles in Figure 4 represent this number as a fraction of *Hipparcos* stars.

Since nearly all of the high-precision Doppler surveys have apparent magnitude-limited target lists (often $V < 7.5$), we investigate the effect that this has on the total target fraction as a function of distance. The fraction of stars having an apparent magnitude V brighter (lower) than a given value are shown by the five dotted lines for $V < 7.5$–9.5. For a survey magnitude-limited to $V = 7.5$, 80% of the Sun-like *Hipparcos* stars will be observable between 0 and 25 pc. This rapidly drops to only 20% for stars between 48 and 50 pc. Thus, the major reason why the target fraction drops with increasing distance is that the stars become too faint for the high-precision Doppler surveys to monitor. The fact that the target fraction (*triangles*) lies near the $V < 8.0$ line indicates that on average $V \sim 8.0$ is the effective limiting magnitude of the targets monitored by the eight combined high-precision Doppler surveys.

In Figure 1, 80 (= 464–384), or 17%, of *Hipparcos* Sun-like stellar systems are not present in any of the Doppler target lists. The triangles in Figure 1 indicate that the ones left out are spread more or less evenly in $B - V$ space spanned by the gray parallelogram. Similarly in Figure 2, 1295 (= 3296–2001), or 39%, are not included in any Doppler target list, but the triangles show that more K stars than FG stars have not been selected, again pointing out that the lower K dwarf stellar brightness is the dominant reason for the lower target fraction, not an effect strongly biased with respect to one set of companions over another.

In the Sun-like region of Figure 1 we use the target number (384) as the mother population for planets and brown dwarfs and the *Hipparcos* number (464) as the mother population for stars. To achieve the same normalizations for planetary, brown dwarf, and stellar companions we assume that the fraction of these 384 targets that have exoplanet or brown dwarf companions is representative of the fraction of the 464 *Hipparcos* stars that have exoplanet or brown dwarf companions. Thus, we renormalize the planetary and brown dwarf companions that have the target sample as their mother population to the *Hipparcos* sample by 464/384 = 1.21 ("renormalization"). Since close-orbiting stellar companions are anticorrelated with close-orbiting substellar companions and the 384 have been selected to exclude separations of $<2''$, the results from the sample of 384 may be a slight overestimate of the relative frequency of substellar companions. However, this overestimate will be less than $\sim$11%, because this is the frequency of close-orbiting stellar secondaries.

A nonoverlapping sample of the eight high-precision Doppler surveys (Lineweaver & Grether 2003) is used as the exoplanet target list; the Elodie target list was kindly provided by C. Perrier (2004, private communication) and additional information to construct the Coralie target list from the *Hipparcos* catalog was obtained from S. Udry (2004, private communication). The Keck and Lick target lists are those of Nidever et al. (2002), since $\sim$7% of the targets in Wright et al. (2004) have not been observed over the full 5 yr baseline used in this analysis. For more details about the sample sizes, observational durations, selection criteria, and sensitivities of the eight surveys see Table 4 of Lineweaver & Grether (2003).

2.2. *Companion Detection and Selection Effects*

The companions to the above Sun-like sample of host stars have primarily been detected using the Doppler technique (but not exclusively high-precision exoplanet Doppler surveys), with some of the stellar pairs also being detected as astrometric or visual binaries. Thus, we need to consider the selection effects of the Doppler method in order to define a less biased sample of companions (Lineweaver & Grether 2003). As a consequence of the exoplanet surveys' limited monitoring duration, we only select those companions with an orbital period $P < 5$ yr. To reduce the selection effect due to the Doppler sensitivity we also limit our less biased sample to companions of mass $M_2 > 0.001\ M_\odot$.

Figure 5 shows all of the Doppler companions to the Sun-like 25 and 50 pc samples within the mass and period range considered here. Our less biased companions are enclosed by the thick solid rectangle. Given a fixed number of targets, the "detected" region should contain all companions that will be found for this region of mass-period space. The "being detected" region should contain some but not all companions that will be found in this region and the "not detected" region contains no companions since the current Doppler surveys are either not sensitive enough or have not been observing for a long enough duration. To avoid the incomplete "being detected" region we limit our sample of companions to $M_2 > 0.001\ M_\odot$. In

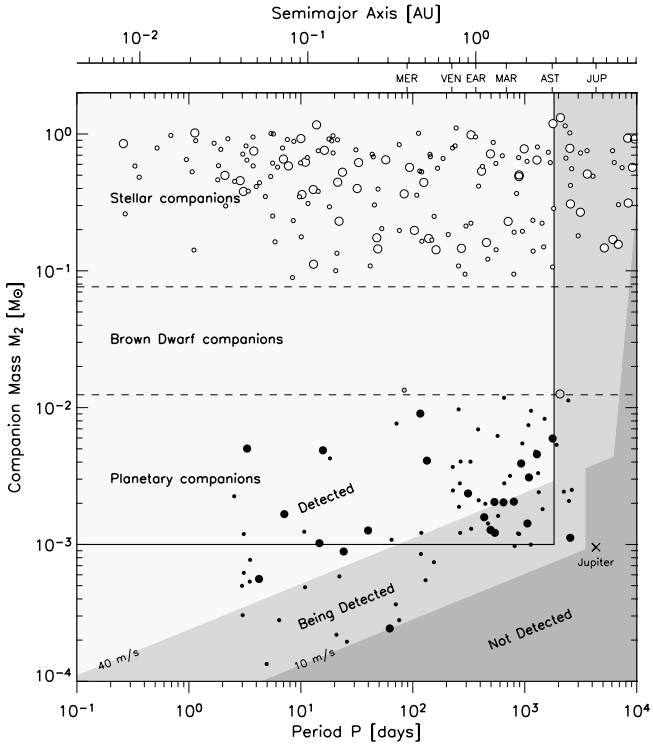

FIG. 5.—Brown dwarf desert in mass and period. Estimated companion mass M_2 vs. orbital period for the companions to Sun-like stars of our two samples: companions with hosts closer than 25 pc (*large symbols*) and those with hosts closer than 50 pc, excluding those closer than 25 pc (*small symbols*). The companions in the thick solid rectangle are defined by periods $P < 5$ yr and masses $10^{-3} < M_2 \lesssim M_\odot$ and form our less biased sample of companions. The stellar (*open circles*), brown dwarf (*gray circles*) and planetary (*filled circles*) companions are separated by dashed lines at the hydrogen and deuterium burning onset masses of $80M_J$ and $13M_J$, respectively. This plot clearly shows the brown dwarf desert for the $P < 5$ yr companions. Planets are more frequent at larger periods than at shorter periods (see Fig. 6). The "detected," "being detected," and "not detected" regions of the mass-period space show the extent to which the high-precision Doppler method is currently able to find companions (Lineweaver & Grether 2003). See the Appendix for discussion of M_2 mass estimates.

Lineweaver et al. (2003) we describe a crude method for making a completeness correction for the lower right corner of the solid rectangle falling within the "being detected" region. The result for the $d < 25$ pc sample is a one-planet correction to the lowest mass bin and for the $d < 50$ pc sample, a six-planet correction to the lowest mass bin (see Table 2, footnote c). Figure 6 shows a projection of Figure 5 onto the period axis. Planets are more clumped toward higher periods than are stellar companions. The Doppler planet detection method is not biased against short period planets. The Doppler stellar companion detections are not significantly biased for shorter periods or against longer periods in our samples' analysis range (period <5 yr) since Doppler instruments of much lower precision than those used to detect exoplanets are able to detect any Doppler companions of stellar mass. Thus, this represents a real difference in period distributions between stellar and planetary companions.

The companions in Figure 5 all have radial velocity (Doppler) solutions. Some of the companions also have additional photometric, interferometric, astrometric, or visual solutions. The exoplanet Doppler orbits are taken from the Extrasolar Planets Catalog (Schneider 2005). Only the planet orbiting the star HIP 108859 (HD 209458) has an additional photometric solution, but this companion falls outside our less biased region ($M_2 < M_J$). For the stellar companion data, the single-lined (SB1) and

TABLE 2

Hipparcos Sample, Doppler Targets, and Detected Companions for Near and Far Samples

		Doppler Target		Companions					
							Stars		
Sample	*Hipparcos* Number	Number	Percent[a]	Total	Planets	BDs	Total	SB1	SB2
$d < 25$ pc	1509	627	42%	...	22	...	...	...	...
Sun-like	464	384	83%	59 (+15)[b]	19 (+1,[c] +4[d])	0	40 (+7,[e] +3[f])	25 (9)[g]	15 (8)[g]
Decl. $< 0°$	211	211	100%	20 (+10)[b]	10	0	10 (+7,[e] +3[f])	8 (3)[g]	2 (1)[g]
Decl. $\geq 0°$	253	173	68%	39	9	0	30	17 (6)[g]	13 (7)[g]
$d < 50$ pc	6924	2351	34%	...	58	...	...	...	...
Sun-like	3296	2001	61%	198 (+80)[b]	54 (+6,[c] +19[f])	1[h]	143 (+14,[e] +41[f])	90 (18)[g]	53 (12)[g]
Decl. $<0°$	1647	1525	93%	72 (+74)[b]	33 (+19)[f]	0	39 (+14,[e] +41[f])	27 (7)[g]	12 (2)[g]
Decl. $\geq 0°$	1649	476	29%	126	21	1	104	63 (11)[g]	41 (10)[g]

[a] Percentage of *Hipparcos* stars that are Doppler targets.
[b] Total of corrections c through to f.
[c] Completeness correction in the lowest mass bin for the lower right corner of our sample in Fig. 5 lying in the "being detected" region (see Lineweaver et al. 2003).
[d] Renormalization for planetary target population (384) being less than stellar companion mother population (464) (see discussion in § 2.1).
[e] Correction based on the most likely scenario that the southern stellar companions from Jones et al. (2002) have periods <5 yr.
[f] Correction for north-south declination asymmetry in companion fraction after correcting for Jones et al. (2002) detections (see § 2.2).
[g] Number of these spectroscopic binaries with an additional astrometric or visual solution (see Appendix).
[h] Result from assuming $\langle \sin i \rangle = 0.785$ when i is unknown (see caption of Fig. 7 and the Appendix).

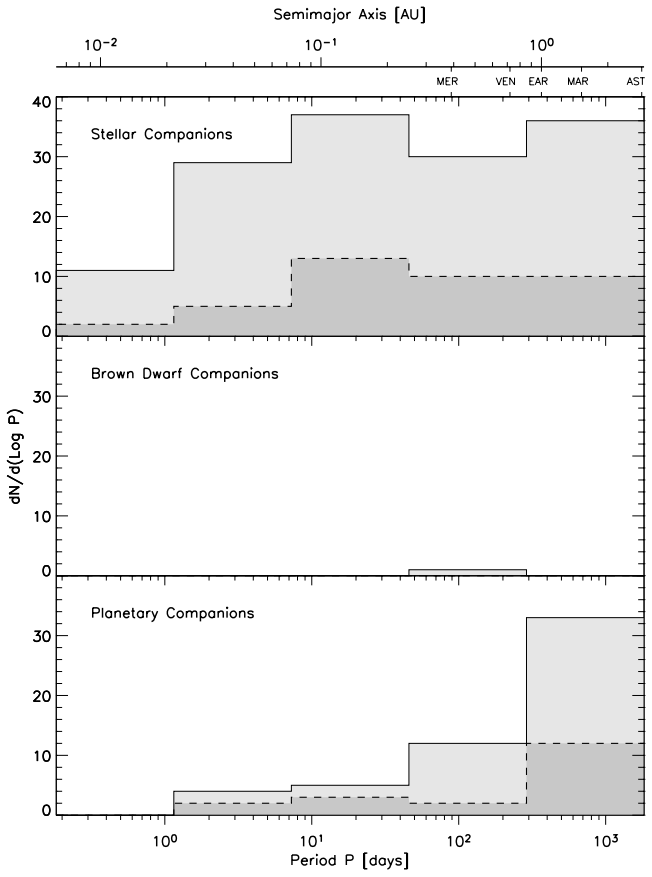

Fig. 6.—Projection of Fig. 5 onto the period axis for the 25 (*dark gray*) and 50 pc (*light gray*) samples. Planets are more clumped toward higher periods than are stellar companions. This would be a selection effect with no significance if the efficiency of finding short period stellar companions with the low-precision Doppler technique used to find spectroscopic binaries, was much higher than the efficiency of finding exoplanets with high-precision spectroscopy. Konacki et al. (2004) and Pont et al. (2004) conclude that the fact that the transit photometry method has found planets in sub-2.5 day periods (while the Doppler method has found none) is due to higher efficiency for small periods and many more target stars and thus that these two observations do not conflict. Thus, there seems to be a real difference in the period distributions of stellar and planetary companions.

double-lined (SB2) spectroscopic binary orbits are primarily from the Ninth Catalog of Spectroscopic Binary Orbits (Pourbaix et al. 2004) with additional interferometric, astrometric, or visual solutions from the Sixth Catalog of Orbits of Visual Binary Stars (Washington Double Star Catalog; Hartkopf & Mason 2004). Many additional SB1s come from Halbwachs et al. (2003). Stellar binaries and orbital solutions also come from Endl et al. (2004), Halbwachs et al. (2000), Mazeh et al. (2003), Tinney et al. (2001), Jones et al. (2002), Vogt et al. (2002), and Zucker & Mazeh (2001a).

We examine the inclination distribution for the 30 Doppler companions ($d < 50$ pc) with an astrometric or visual solution. We find that 24 of these 30 companions have a minimum mass larger than $80M_J$ (Doppler stellar candidates) and that six of these 30 companions have a minimum mass between $13M_J$ and $80M_J$ (Doppler brown dwarf candidates). These six Doppler brown dwarf candidates are a subset of the 16 Doppler brown dwarf candidates in the far sample that have an astrometric orbit derived with a confidence level greater than 95% from *Hipparcos* measurements (Halbwachs et al. 2000; Zucker & Mazeh 2001a) and are thus assumed to have an astrometric orbit.

As shown in Figure 7, the inclination distribution is approximately random for the 24 companions with a minimum mass in the stellar regime, whereas it is biased toward low inclinations for the six companions in the brown dwarf regime. All six of the Doppler brown dwarf candidates with an astrometric determination of their inclination have a true mass in the stellar regime. This includes all three of the Doppler brown dwarf candidates that are companions to stars in our close sample ($d < 25$ pc), thus leaving an empty brown dwarf regime. Also shown in Figure 7 is the distribution of the maximum values of $\sin i$ that would put the true masses of the remaining 10 Doppler brown dwarf candidates with unknown inclinations in the stellar regime. This distribution is substantially less biased than the observed $\sin i$ distribution, strongly suggesting that the remaining 10 Doppler brown dwarf candidates will also have masses in the stellar regime. Thus, astrometric corrections leave us with no solid candidates with masses in the brown dwarf regime from the 16 Doppler brown dwarf candidates in the far sample ($d < 50$ pc), consistent with the result obtained for the close sample.

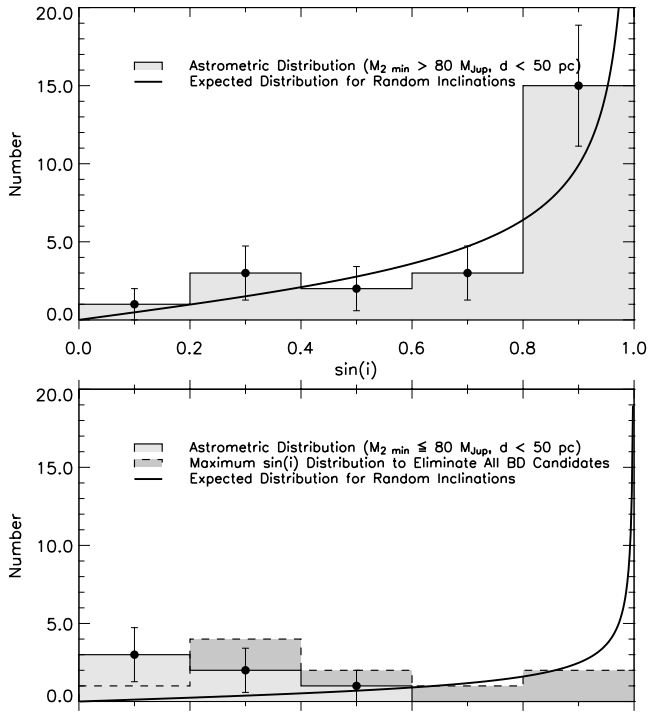

FIG. 7.—Astrometric inclination distribution for close companions ($d < 50$ pc) with a minimum mass larger than $80M_J$ (Doppler stellar candidates; *top*) and between $13M_J$ and $80M_J$ (Doppler brown dwarf candidates; *bottom*). There are 24 companions with astrometric solutions and a minimum mass in the stellar regime and six with a minimum mass in the brown dwarf regime. The inclination distribution is approximately random for companions with a minimum mass in the stellar regime whereas it is biased toward low inclinations for companions in the brown dwarf regime. All six astrometric determinations of $\sin i$ for brown dwarf candidates put their true mass in the stellar regime. Also shown is the distribution of the maximum values of $\sin i$ that would place the true masses of the remaining 10 brown dwarf candidates without astrometric or visual solutions in the stellar regime. A distribution less biased than the observed $\sin i$ distribution would be required. This strongly suggests that the 10 candidates without astrometric or visual solutions will also have masses in the stellar regime. Therefore, astrometric corrections leave us with no solid candidates with masses in the brown dwarf region. Two weak brown dwarf candidates are worth mentioning. HD 114762 has a minimum mass below $13M_J$. However, to convert minimum mass to mass, we have assumed random inclinations and have used $\langle \sin i \rangle \approx 0.785$. This conversion puts the estimated mass of HD 114762 in the brown dwarf regime ($M \gtrsim 13M_J$). In Fig. 5, this is the only companion lying in the brown dwarf regime. Another weak brown dwarf candidate is the only candidate that requires a $\sin i < 0.2$ to place its mass in the stellar regime.

The size of the 25 and 50 pc samples, the extent to which they are being targeted for planets, and the number and types of companions found, along with any associated corrections, are summarized in Table 2. For the stars closer than 25 pc, 59 have companions in the less biased region (*rectangle circumscribed by thick line*) of Figure 5. Of these, 19 are exoplanets, 0 are brown dwarfs, and 40 are of stellar mass. Of the stellar companions, 25 are SB1s and 15 are SB2s. For the stars closer than 50 pc, 198 have companions in the less biased region. Of these, 54 are exoplanets, 1 is a brown dwarf, and 143 are stars. Of the stellar companions, 90 are SB1s and 53 are SB2s.

We find an asymmetry in the north-south declination distribution of the Sun-like stars with companions, probably due to undetected or unpublished stellar companions in the south. The number of hosts closer than 25 pc with planetary or brown dwarf companions are symmetric in north-south declination to within 1 σ Poisson error bars, but because more follow-up work has been done in the north, more of the hosts with stellar companions with orbital solutions are in the northern hemisphere (30) than the southern hemisphere (10). A comparison of our northern sample of hosts with stellar companions to the similarly selected approximately complete sample of Halbwachs et al. (2003) indicates that our 25 pc northern sample of hosts with stellar companions is also approximately complete. Under this assumption, the number of stellar companions missing from the south can be estimated by making a minimal correction up to the 1 σ error level below the expected number, based on the northern follow-up results. Of the 464 Sun-like stars closer than 25 pc, 211 have a southern declination (decl. $< 0^\circ$) and 253 have a northern declination (decl. $\geq 0^\circ$), and thus $\sim$25 (25/211 $\approx$ 30/253) stars in the south should have a stellar companion when fully corrected or 20 if we make a minimal correction. Thus, we estimate that we are missing at least $\sim$10 (= 20−10) stellar companions in the south, seven of which have been detected by Jones et al. (2002) under the plausible assumption that the orbital periods of the companions detected by Jones et al. (2002) are less than 5 yr. Although these seven SB1 stellar companions detected by Jones et al. (2002) have as yet no published orbital solutions, we assume that the SB1 stellar companions detected by Jones et al. (2002) have $P < 5$ yr since they have been observed as part of the high Doppler precision program at the Anglo-Australian Observatory (started in 1998) for a duration of less than 5 yr before being announced. The additional estimated stellar companions are assumed to have the same mass distribution as the other stellar companions.

We can similarly correct the declination asymmetry in the sample of Sun-like stars closer than 50 pc. We find that there should be, after a minimal correction, an additional 55 stars that are stellar companion hosts in the southern hemipshere. Fourteen of these 55 stellar companions are assumed to have been detected by Jones et al. (2002). An asymmetry found in the planetary companion fraction in the 50 pc sample due to the much larger number of stars being monitored less intensively for exoplanets in the south ($\sim$2% = 33/1525) compared to the north ($\sim$4% = 21/476) results in a correction of 19 planetary companions in the south. The results given in Table 3 are done both with and without the asymmetry corrections.

Unlike the 25 pc sample for which we are confident that the small corrections made to the number of companions will result in a reliable estimate of a census, correcting the 50 pc sample for the large number of missing companions is less reliable. This is so because if it were complete, the 50 pc sample would have approximately 8 times the number of companions as the 25 pc sample, since the 50 pc sample has 8 times the volume of the 25 pc sample. However, the incomplete 50 pc sample has only $\sim$7 (= 3296/464) times the number of *Hipparcos* stars, $\sim$5(= 2001/384) times as many exoplanet targets and $\sim$3 times as many companions as the 25 pc sample. Thus, rather than correcting both planetary and stellar companions by large amounts, we show in § 3 that the relative number and distribution of the observed planetary and stellar companions (plus a small completeness correction for the "being detected" region of six planets and an additional 14 probable stellar companions from Jones et al. [2002]; see Table 2) remains approximately unchanged when compared to the corrected companion distribution of the 25 pc sample. Analyses both with and without a correction for the north-south asymmetry produce similar results for the brown dwarf desert (Table 3).

3. COMPANION MASS FUNCTION

The close companion mass function to Sun-like stars clearly shows a brown dwarf desert for both the 25 pc (Fig. 8) and the 50 pc (Fig. 9) samples. The numbers of both the planetary and stellar mass companions decrease toward the brown dwarf mass

TABLE 3
COMPANION SLOPES AND COMPANION DESERT MASS MINIMA

Sample	Asymmetry Correction	Figure	LHS Slope	RHS Slope	Slope Minima[a] [M_J]
$d < 25$ pc	Yes	8	-15.2 ± 5.6	22.0 ± 8.8	31^{+25}_{-18}
$d < 25$ pc	No		-15.2 ± 5.6	20.7 ± 8.5	30^{+25}_{-17}
$d < 50$ pc	Yes		-9.4 ± 3.0	24.3 ± 4.6	44^{+15}_{-24}
$d < 50$ pc	No	9	-9.1 ± 2.9	24.1 ± 4.7	43^{+14}_{-23}
$d < 25$ pc and $M_1 < 1\ M_\odot$	Yes	10	-17.5 ± 5.4	19.4 ± 10.7	18^{+17}_{-9}
$d < 50$ pc and $M_1 < 1\ M_\odot$	No	11	-5.9 ± 5.1	25.2 ± 11.4	39^{+9}_{-23}
$d < 25$ pc and $M_1 \geq 1\ M_\odot$	Yes	10	-12.4 ± 9.2	20.0 ± 10.9	50^{+28}_{-26}
$d < 50$ pc and $M_1 \geq 1\ M_\odot$	No	11	-12.2 ± 8.2	21.1 ± 10.4	45^{+21}_{-21}

[a] Values of mass where the best-fitting lines to the LHS and RHS intersect. The errors given are from the range between the two intersections with the abscissa.

range. Both plots contain the detected Doppler companions, shown as the gray histogram, within our less biased sample of companions ($P < 5$ yr and $M_2 > 10^{-3}\ M_\odot$; see § 2.2). The hatched histograms at large mass show the subset of the stellar companions that are not included in any of the exoplanet Doppler surveys. A large bias against stellar companions would have been present if we had only included companions found by the exoplanet surveys. For multiple-companion systems, we select the most massive companion in our less biased sample to represent the system. We put the few companions (three in the 25 pc sample, six in the 50 pc sample) that have a mass slightly larger than 1 $M_\odot$ in the largest mass bin in the companion mass distributions.

Fitting straight lines using a weighted least-squares method to the three bins on the left-hand side (LHS) and right-hand side (RHS) of the brown dwarf region of the mass histograms (Figs. 8 and 9) gives us gradients of -15.2 ± 5.6 (LHS) and 22.0 ± 8.8 (RHS) for the 25 pc sample and -9.1 ± 2.9 (LHS) and 24.1 ± 4.7 (RHS) for the 50 pc sample. Since the slopes

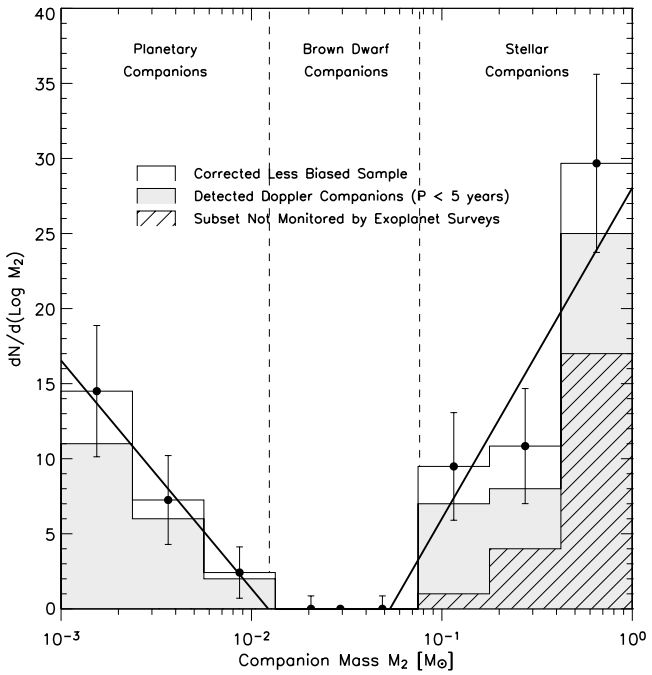

FIG. 8.—Brown dwarf desert in close sample. Histogram of the companions to Sun-like stars closer than 25 pc plotted against mass. The gray histogram is made up of Doppler-detected companions in our less biased ($P < 5$ yr and $M_2 > 10^{-3}\ M_\odot$) sample. The corrected version of this less biased sample includes an extra seven probable SB1 stars from (Jones et al. 2002; see Table 2, footnote e) and three extra stars from an asymmetry in the host declination distribution (Table 2, footnote f). The planetary mass companions are also renormalized to account for the small number of *Hipparcos* Sun-like stars that are not being Doppler monitored (21% renormalization; Table 2, footnote d) and a one-planet correction for the undersampling of the lowest mass bin due to the overlap with the "being detected" region (Table 2, footnote c). The hatched histogram is the subset of detected companions to hosts that are not included on any of the exoplanet search target lists and hence shows the extent to which the exoplanet target lists are biased against the detection of stellar companions. Since instruments with a radial velocity sensitivity $K_S \leq 40$ m s^{-1} (see eq. [2] of Appendix) were used for all the companions, we expect no other substantial biases to affect the relative amplitudes of the stellar companions on the RHS and the planetary companions on the LHS. The brown dwarf mass range is empty.

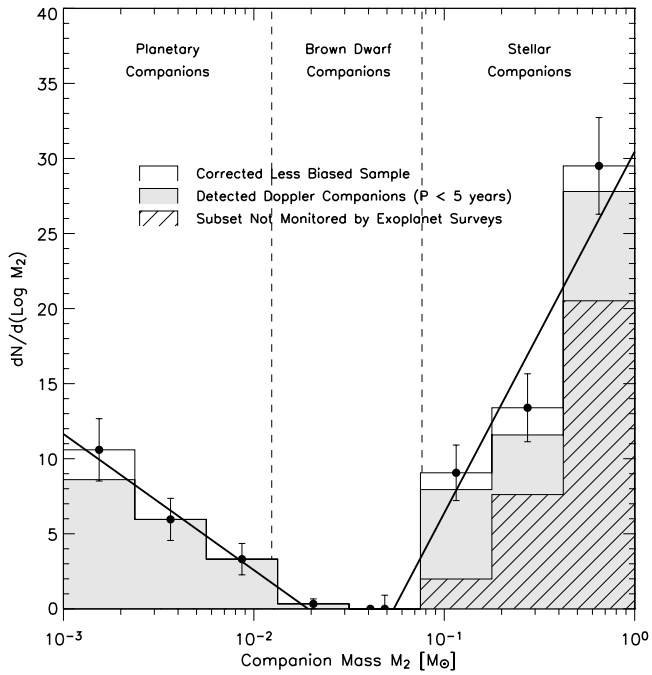

FIG. 9.—Same as Fig. 8, but for the larger 50 pc sample renormalized to the size of the 25 pc sample. Fitting straight lines using a weighted least-squares fit to the three bins on the LHS and RHS gives us gradients of -9.1 ± 2.9 and 24.1 ± 4.7, respectively (*solid lines*). Hence, the brown dwarf desert is significant at more than the 3 σ level. These LHS and RHS slopes agree to within about 1 σ of those in Fig. 8. The ratio of the number of companions on the LHS to the RHS is also about the same for both samples. Hence, the relative number and distribution of companions is approximately the same as in Fig. 8. The separate straight line fits to the three bins on the LHS and RHS intersect at $M = 43^{+14}_{-23} M_J$ beneath the abscissa. Approximately 16% of the stars have companions in our less biased region. Of these, $4.3\% \pm 1.0\%$ have companions of planetary mass, $0.1^{+0.2}_{-0.1}\%$ have brown dwarf companions, and $11.2\% \pm 1.6\%$ have companions of stellar mass. We renormalize the mass distribution in this figure by comparing each bin in this figure with its corresponding bin in Fig. 8 and scaling the vertical axis of Fig. 9 so that the difference in height between the bins is on average a minimum. We find that the optimum renormalization factor is 0.33. This plot does not include the asymmetry correction for the planetary and stellar companions discussed in § 2.2 and shown in Table 2.

TABLE 4
Companion Fraction Comparison

Sample	Asymmetry Correction	Figure	Total (%)	Planetary (%)	Brown Dwarf (%)	Stellar (%)
$d < 25$ pc	Yes	8	16.0 ± 5.2	5.2 ± 1.9	$0.0^{+0.4}_{-0.0}$	10.8 ± 2.9
$d < 25$ pc	No		15.3 ± 5.0	5.2 ± 1.9	$0.0^{+0.4}_{-0.0}$	10.1 ± 2.7
$d < 50$ pc	Yes		15.6 ± 2.8	4.4 ± 1.0	$0.1^{+0.2}_{-0.1}$	11.1 ± 1.6
$d < 50$ pc	No	9	15.6 ± 2.8	4.3 ± 1.0	$0.1^{+0.2}_{-0.1}$	11.2 ± 1.6
$d < 25$ pc and $M_1 < 1\ M_\odot$	Yes	10	16.0 ± 5.8	4.2 ± 1.9	$0.0^{+0.4}_{-0.0}$	11.8 ± 3.5
$d < 50$ pc and $M_1 < 1\ M_\odot$	No	11	15.6 ± 6.0	2.6 ± 1.7	$0.2^{+0.4}_{-0.2}$	12.8 ± 3.9
$d < 25$ pc and $M_1 \geq 1\ M_\odot$	Yes	10	16.0 ± 7.0	6.6 ± 3.1	$0.0^{+0.4}_{-0.0}$	9.4 ± 3.5
$d < 50$ pc and $M_1 \geq 1\ M_\odot$	No	11	15.6 ± 6.7	6.2 ± 2.9	$0.0^{+0.4}_{-0.0}$	9.4 ± 3.4

have opposite signs, they form a valley that is the brown dwarf desert. The presence of a valley between the negative and positive sloped lines is significant at more than the 3 σ level. The ratio of the corrected number of companions in the less biased sample on the LHS to the RHS along with their poisson error bars is $(24 \pm 9)/(50 \pm 13) = 0.48 \pm 0.22$ with no companions in the middle two bins for the 25 pc sample. For the larger 50 pc sample the corrected less biased LHS/RHS ratio is $(60 \pm 14)/(157 \pm 22) = 0.38 \pm 0.10$, with one brown dwarf companion in the middle two bins. Thus, the LHS and RHS slopes agree to within about 1 σ and so do the LHS/RHS ratios, indicating that the companion mass distribution for the larger 50 pc sample is not significantly different from the more complete 25 pc sample and that the relative fraction of planetary, brown dwarf, and stellar companions is approximately the same. A comparison of the relative number of companions in each bin in Figure 8 with its corresponding bin in Figure 9 produces a best fit of $\chi^2 = 1.9$.

To find the driest part of the desert, we fit separate straight lines to the three bins on either side of the brown dwarf desert (*solid lines*) in Figures 8 and 9. The deepest part of the valley where the straight lines cross beneath the abscissa is at $M = 31^{+25}_{-18} M_J$ and $M = 43^{+14}_{-23} M_J$ for the 25 and 50 pc samples, respectively. These results are summarized in Table 3. The driest part of the desert is virtually the same for both samples, even though we see a bias in the stellar binarity fraction of the 50 pc sample (Fig. 3). We have done the analysis with and without the minimal declination asymmetry correction. The position of the brown dwarf minimum and the slopes are robust to this correction (see Table 3).

The smaller 25 pc Sun-like sample contains 464 stars, with $16.0\% \pm 5.2\%$ of these having companions in our corrected less biased sample. Of these $\sim$16% with companions, $5.2\% \pm 1.9\%$ are of planetary mass and $10.8\% \pm 2.9\%$ are of stellar mass. None is of brown dwarf mass. This agrees with previous estimates of stellar binarity such as that found by Halbwachs et al. (2003) of 14% for a sample of G-dwarf companions with a slightly larger period range ($P < 10$ yr). The planet fraction agrees with the fraction $4\% \pm 1\%$ found in Lineweaver & Grether (2003) when most of the known exoplanets are considered. The 50 pc sample has a large incompleteness due to the lower fraction of monitored stars (Fig. 4), but as shown above, the relative number of companion planets, brown dwarfs, and stars is approximately the same as for the 25 pc sample. The 50 pc sample has a total companion fraction of $15.6\% \pm 2.8\%$, where $4.3\% \pm 1.0\%$ of the companions are of planetary mass, $0.1^{+0.2}_{-0.1}\%$ are of brown dwarf mass, and $11.2\% \pm 1.6\%$ are of stellar mass. Table 4 summarizes these companion fractions.

Surveys of the multiplicity of nearby Sun-like stars yield the relative numbers of single, double, and multiple star systems. According to Duquennoy & Mayor (1991), 51% of star systems are single stars, 40% are double-star systems, 7% are triple, and 2% are quadruple or more. Of the 49% (=40 + 7 + 2) that are stellar binaries or multiple star systems, 11% have stellar companions with periods less than 5 yr, and thus we can infer that the remaining 38% have stellar companions with $P > 5$ yr. Among the 51% without stellar companions, we find that $\sim$5% have close ($P < 5$ yr) planetary companions with $1 < M/M_J < 13$, while <1% have close brown dwarfs companions.

The Doppler method should preferentially find planets around lower mass stars where a greater radial velocity is induced. This is the opposite of what is observed as shown in Figures 10 and 11, where we split the 25 and 50 pc samples, respectively, into companions to hosts with masses above and below 1 $M_\odot$. We scale these smaller samples to the size of the full 25 and 50 pc samples (Figs. 8 and 9, respectively). The Doppler technique is also a function of $B - V$ color (Saar et al. 1998), with the level of systematic errors in the radial velocity measurements decreasing as we move from high mass to low mass ($B - V = 0.5$–1.0) through our two samples, peaking for late K spectral type stars before increasing for the lowest mass M-type stars again. Hence, again finding planets around the lower mass stars (early K spectral type) in our sample should be easier.

3.1. *Comparison with Other Results*

Although there are some similarities, the companion mass function found by Heacox (1999), Zucker & Mazeh (2001b), and Mazeh et al. (2003) is different from that shown in Figures 8 and 9. Our approach was to normalize the companion numbers to a well-defined subsample of *Hipparcos* stars, whereas these authors use two different samples of stars, one to find the planetary companion mass function and another to find the stellar companion mass function, which are then normalized to each other. The different host star properties and levels of completeness of the two samples may make this method more prone than our method to biases in the frequencies of companions.

Both Heacox (1999) and Zucker & Mazeh (2001b) combined the companions of the stellar mass sample of Duquennoy & Mayor (1991) with the known substellar companions but identified different mass functions for the planetary mass regime below $10 M_J$ and similar flat distributions in logarithmic mass for brown dwarf and stellar mass companions. Heacox (1999) found that the logarithmic mass function in the planetary regime is best fit by a power law ($dN/d \log M \propto M^\Gamma$) with index Γ between 0 and -1, whereas Zucker & Mazeh (2001b) find an approximately flat distribution (power law with index 0). Our work here and in Lineweaver & Grether (2003) suggests that neither the stellar nor the planetary companion distributions are flat ($\Gamma = -0.7$). Rather, they both slope down toward the brown dwarf desert, more in agreement with the results of Heacox (1999).

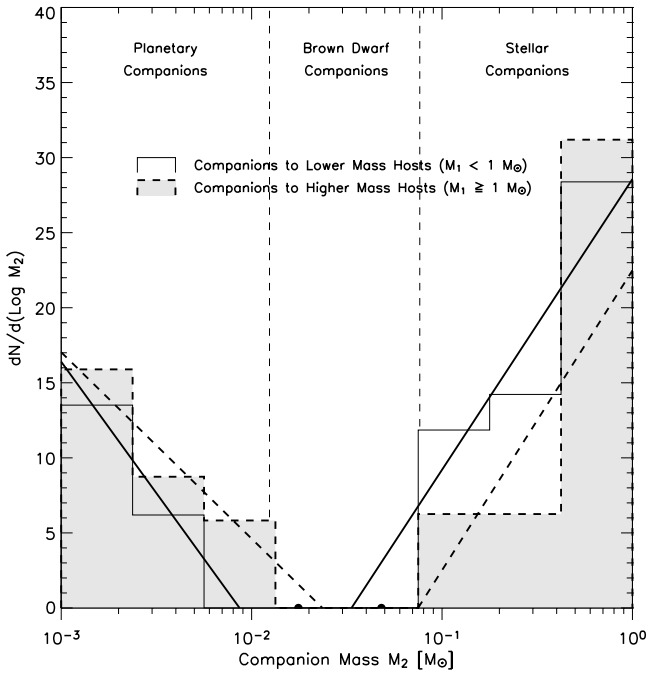

FIG. 10.—Same as Fig. 8, but for the 25 pc sample split into companions to lower mass hosts ($M_1 < 1\ M_\odot$) and companions to higher mass hosts ($M_1 \geq 1\ M_\odot$). The lower mass hosts have 4.2% planetary, 0.0% brown dwarf, and 11.8% stellar companions. The higher mass hosts have 6.6% planetary, 0.0% brown dwarf, and 9.4% stellar companions. The Doppler method should preferentially find planets around lower mass stars where a greater radial velocity is induced. This is the opposite of what we observe. To aid comparison, both samples are scaled such that they contain the same number of companions as the full corrected less biased 25 pc sample of Fig. 8.

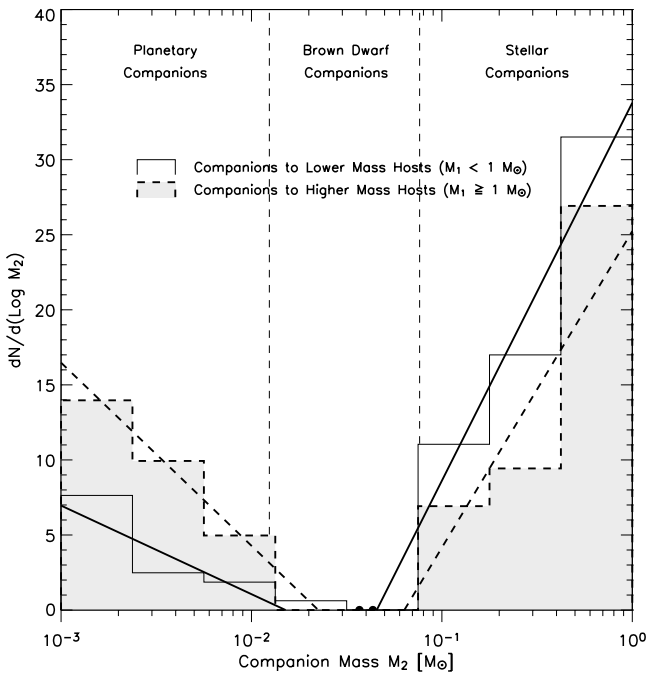

FIG. 11.—Same as Fig. 9, but for the 50 pc sample split into companions to lower mass hosts ($M_1 < 1\ M_\odot$) and companions to higher mass hosts ($M_1 \geq 1\ M_\odot$). Both samples are scaled such that they contain the same number of companions as the corrected less biased 50 pc sample of Fig. 9. Also shown are the linear best fits to the planetary and stellar companions of the two populations.

The work most similar to ours is probably that of Mazeh et al. (2003), who looked at a sample of main-sequence stars with primaries in the range 0.6–0.85 $M_\odot$ and $P < 3000$ days using infrared spectroscopy and combined them with the known substellar companions of these main-sequence stars and found that in logarithmic mass the stellar companions reduce in number toward the brown dwarf mass range. This agrees with our results for the shape of the stellar mass companion function. However, they identify a flat distribution for the planetary mass companions in contrast to our nonzero slope (see Table 3). Mazeh et al. (2003) found the frequency of stellar and planetary companions ($M_2 > 1 M_J$) to be 15% (for stars below 0.7 $M_\odot$) and 3%, respectively. This compares with our estimates of 8% (for stars below 0.7 $M_\odot$) and 5%. The larger period range used by Mazeh et al. (2003) can account for the difference in stellar companion fractions.

4. COMPARISON WITH THE INITIAL MASS FUNCTION

Brown dwarfs found as free-floating objects in the solar neighborhood and as members of young star clusters have been used to extend the initial mass function (IMF) well into the brown dwarf

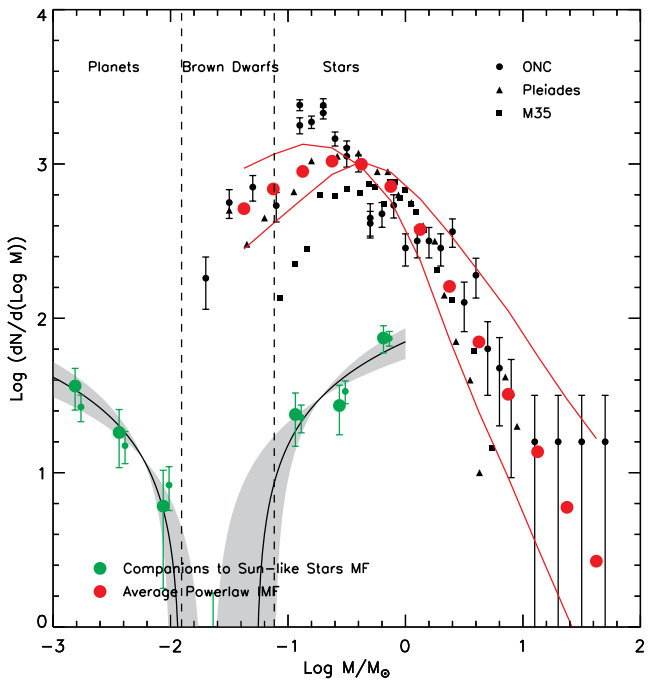

FIG. 12.—Mass function of companions to Sun-like stars (*lower left*) compared to the initial mass function (IMF) of cluster stars (*upper right*). Our mass function of the companions to Sun-like stars is shown by the green dots (*larger dots*, $d < 25$ pc sample; *smaller dots*, $d < 50$ pc sample). The linear slopes we fit to the data in Fig. 8 are also shown along with their error. Data for the number of stars and brown dwarfs in the Orion Nebula Cluster (ONC) (*circles*), Pleiades cluster (*triangles*), and M35 cluster (*squares*) come from Hillenbrand & Carpenter (2000), Slesnick et al. (2004), Moraux et al. (2003), and Barrado y Navascues et al. (2001), respectively, and are normalized such that they overlap for masses larger than 1 $M_\odot$ where a single power-law slope applies. The absolute normalization of cluster stars is arbitrary, while the companion mass function is normalized to the IMF of the cluster stars by scaling the three companion points of stellar mass to be on average ~7% for $P < 5$ yr (derived from the stellar multiplicity of Duquennoy & Mayor [1991] discussed in § 3, combined with our estimate that 11% of Sun-like stars have stellar secondaries). The average power-law IMF derived from various values of the slope of the IMF quoted in the literature (Hillenbrand 2004) is shown as larger red dots along with two thin red lines showing the rms error. If the turn-down in the number of brown dwarfs of the IMF is due to a selection effect because it is hard to detect brown dwarfs, then the two distributions are even more different from each other. For clarity, the smaller green dots are shifted slightly to the right.

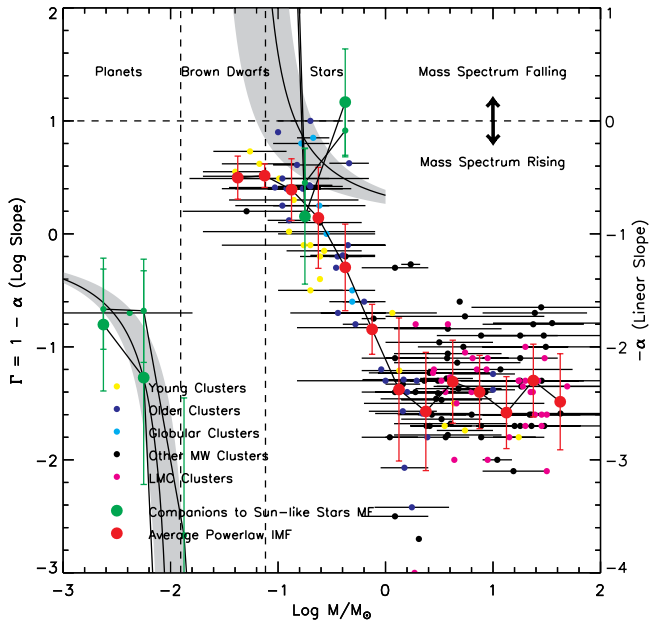

FIG. 13.—IMF for clusters represented by a series of power-law slopes (Hillenbrand 2004). Each point represents the power-law slope claimed to apply within the mass range indicated by the horizontal lines. Although the IMF is represented by a series of power laws, the IMF is not a power law for masses less than 1 $M_\odot$ where the slope continually changes. The green dots show the slope of the companion mass function to Sun-like stars between the bins of Figs. 8 and 9 with the larger and smaller dots, respectively. The linear fits to the data in Fig. 8 and their associated error are shown by the curves inside the gray regions. The power-law fit of Lineweaver & Grether (2003, shown as the green dot with a horizontal line indicating the range over which the slope applies) is consistent with these fits. The larger red dots with error bars represent the average power-law IMF with a rms error. Γ and $-\alpha$ are the logarithmic and linear slopes of the mass function, respectively. The logarithmic mass power-law distribution is $dN/d\log M \propto M^{\Gamma}$ and the linear mass power-law distribution is $dN/dM \propto M^{-\alpha}$, where $\Gamma = 1 - \alpha$. The errors on the fits of Fig. 8 get smaller at $M \sim 10^{-3}$ and ~ 1 $M_\odot$, since as $\log(M/M_\odot)$ tends to $\pm\infty$, Γ tends to 0. This can also be seen in Fig. 12, where the slopes of the upper and lower contours become increasingly similar.

regime. Comparing the mass function of our sample of close-orbiting companions of Sun-like stars to the IMF of single stars indicates how the environment of a host affects stellar and brown dwarf formation and/or migration. Here we quantify how different the companion mass function is from the IMF (Halbwachs et al. 2000).

The galactic IMF appears to be remarkably universal and independent of environment and metallicity, with the possible exception of the substellar mass regime. A weak empirical trend with metallicity is suggested for very low mass stars and brown dwarfs, where more metal-rich environments may be producing relatively more low-mass objects (Kroupa 2002). This is consistent with an extrapolation up in mass from the trend found in exoplanet hosts. The IMF is often represented as a power law, although this only appears to be accurate for stars with masses above ~ 1 $M_\odot$ (Hillenbrand 2004). The stellar IMF slope gets flatter toward lower masses and extends smoothly and continously into the substellar mass regime, where it appears to turn over.

Free-floating brown dwarfs may be formed either as ejected stellar embryos or from low-mass protostellar cores that have lost their accretion envelopes due to photoevaporation from the chance proximity of a nearby massive star (Kroupa & Bouvier 2003). This hypothesis may explain their occurrence in relatively rich star clusters such as the Orion Nebula cluster and their virtual absence in pre–main-sequence stellar groups such as Taurus Auriga.

In Figures 12 and 13 we compare the mass function of companions to Sun-like stars with the IMF of cluster stars. The mass function for companions to Sun-like stars is shown by the green dots from Figures 8 and 9 (larger dots are the $d < 25$ pc sample and smaller dots are the $d < 50$ pc sample). The linear slopes from Figure 8 and their 1 σ confidence region are also shown. Between $\log(M/M_\odot) \approx -1.0$ and -0.5 ($0.1\ M_\odot < M < 0.3\ M_\odot$) the slopes are similar. However, above 0.3 $M_\odot$ and below 0.1 $M_\odot$ the slopes become inconsistent. Above 0.3 $M_\odot$ the slopes, while of similar magnitude, are of opposite sign, and below 0.1 $M_\odot$ the companion slope is much steeper than the IMF slope. The IMF for young clusters (*yellow dots*) is statistically indistinguishable from that of older stars (*blue dots*) and follows the average IMF.

5. SUMMARY AND DISCUSSION

We analyze the close-orbiting ($P < 5$ yr) planetary, brown dwarf, and stellar companions to Sun-like stars to help constrain their formation and migration scenarios. We use the same sample to extract the relative numbers of planetary, brown dwarf, and stellar companions and verify the existence of a brown dwarf desert. Both planetary and stellar companions reduce in number toward the brown dwarf mass range. We fit the companion mass function over the range that we analyze ($0.001 < M/M_\odot \lesssim 1.0$) by two separate straight lines fit separately to the planetary and stellar data points. The straight lines intersect in the brown dwarf regime, at $M = 31^{+25}_{-18} M_J$. This result is robust to the declination asymmetry correction (Table 3).

The period distribution of close-orbiting ($P < 5$ yr) companion stars is different from that of the planetary companions. The close-in stellar companions are fairly evenly distributed over $\log P$, with planets tending to be clumped toward higher periods. We compare the companion mass function to the IMF for bodies in the brown dwarf and stellar regime. We find that starting at 1 $M_\odot$ and decreasing in mass, stellar companions continue to reduce in number into the brown dwarf regime, while cluster stars increase in number before reaching a maximum just before the brown dwarf regime (Fig. 13). This leads to a difference of at least 1.5 orders of magnitude between the much larger number of brown dwarfs found in clusters and those found as close-orbiting companions to Sun-like stars.

The period distribution of close-orbiting companions may be more a result of post-formation migration and gravitational jostling than representive of the relative number of companions that are formed at a specific distance from their hosts. The companion mass distribution is more fundamental than the period distribution and should provide better constraints on formation models, but our ability to sample the mass distribution is only for $P < 5$ yr.

We show in Figures 10 and 11 that lower mass hosts have more stellar companions and fewer giant planet companions while higher mass hosts have fewer stellar companions but more giant planet companions. The brown dwarf desert is generally thought to exist at close separations $\lesssim 3$ AU (or equivalently $P \leq 5$ yr; Marcy & Butler 2000) but may disappear at wider separations. Gizis et al. (2001) suggest that at very large separations (>1000 AU) brown dwarf companions may be more common. However, McCarthy & Zuckerman (2004) in their observation of 280 GKM stars find only one brown dwarf between 75 and 1200 AU. Gizis et al. (2003) reports that $15\% \pm 5\%$ of M/L dwarfs are brown dwarf binaries with separations in the range 1.6–16 AU. This falls to $5\% \pm 3\%$ of M/L dwarfs with

separations less than 1.6 AU and none with separations greater than 16 AU. This differs greatly from the brown dwarfs orbiting Sun-like stars but is consistent with our host/minimum-companion-mass relationship; i.e., we expect no short period brown dwarf desert around M or L type stars.

Three systems containing both a companion with a minimum mass in the planetary regime and a companion with a minimum mass in the brown dwarf regime are known—HD 168443 (Marcy et al. 2001), HD 202206 (Udry et al. 2002; Correia et al. 2005), and GJ 86 (Queloz et al. 2000; Els et al. 2001). Our analysis suggests that both the M sin i brown dwarfs orbiting HD 168443 and HD 202206 are probably stars (see § 2.2 for our false positive brown dwarf correction). If the M sin i planetary companions in these two systems are coplanar with the larger companions, then these "planets" may be brown dwarfs or even stars. GJ 86 contains a possible brown dwarf detected orbiting at $\sim$20 AU ($P > 5$ yr) and so was not part of our analysis. However, this does suggest that systems containing stars, brown dwarfs, and planets may be possible.

We find that approximately 16% of Sun-like stars have a close companion more massive than Jupiter. Of these 16%, 11% $\pm$ 3% are stellar, $<$1% are brown dwarf, and 5% $\pm$ 2% are planetary companions (Table 4). Although Lineweaver & Grether (2003) show that the fraction of Sun-like stars with planets is greater than 25%, this is for target stars that have been monitored the longest ($\sim$15 yr) and at optimum conditions (stars with low-level chromospheric activity or slow rotation) using the high-precision Doppler method. When we limit the analysis of Lineweaver & Grether (2003) to planetary companions with periods of less than 5 yr and masses larger than Jupiter, we find the same value that we calculate here. When we split our sample of companions into those with hosts above and below 1 $M_\odot$, we find that for the lower mass hosts 11.8% have stellar, $<$1% have brown dwarf, and 4.2% have planetary companions and that for the higher mass hosts 9.4% have stellar, $<$1% have brown dwarf, and 6.6% have planetary companions (Table 4). More massive hosts have more planets and fewer stellar companions than less massive hosts. These are marginal results but are seen in both the 25 and 50 pc samples.

The constraints that we have identified for the companions to Sun-like stars indicate that close-orbiting brown dwarfs are very rare. The fact that there is a close-orbiting brown dwarf desert but no free-floating brown dwarf desert suggests that post-collapse migration mechanisms may be responsible for this relative dearth of observable brown dwarfs rather than some intrinsic minimum in fragmentation and gravitational collapse in the brown dwarf mass regime (Ida & Lin 2004). Whatever migration mechanism is responsible for putting hot Jupiters in close orbits, its effectiveness may depend on the mass ratio of the object to the disk mass. Since there is evidence that disk mass is correlated to host mass, the migratory mechanism may be correlated to host mass, as proposed by Armitage & Bonnell (2002).

We would like to thank Christian Perrier for providing us with the Elodie exoplanet target list, Stephane Udry for addititional information on the construction of the Coralie exoplanet target list, and Lynne Hillenbrand for sharing her data collected from the literature on the power-law IMF fits to various stellar clusters. This research has made use of the SIMBAD database, operated at CDS, Strasbourg, France. This research has made use of the Washington Double Star Catalog maintained at the U.S. Naval Observatory.

APPENDIX

COMPANION MASS ESTIMATES

The Doppler method for companion detection cannot give us the mass of a companion without some additional astrometric or visual solution for the system or by making certain assumptions about the unknown inclination except in the case in which a host star and its stellar companion have approximately equal masses and a double-lined solution is available. Thus, to find the companion mass M_2 that induces a radial velocity K_1 in a host star of mass M_1 we use

$$K_1 = \left(\frac{2\pi G}{P}\right)^{1/3} \frac{M_2 \sin i}{(M_1 + M_2)^{2/3}} \frac{1}{(1 - e^2)^{1/2}} \tag{1}$$

(see Heacox 1999). This equation can be expressed in terms of the mass function $f(m)$:

$$f(m) = \frac{M_2^3 \sin^3(i)}{(M_1 + M_2)^2} = \frac{PK_1^3(1 - e^2)^{3/2}}{2\pi G}. \tag{2}$$

Equation (3) can then be expressed in terms of a cubic equation in the mass ratio $q = M_2/M_1$, where $Y = f(m)/M_1$:

$$q^3 \sin^3(i) - Yq^2 - 2Yq - Y = 0. \tag{3}$$

For planets ($M_1 \gg M_2$) we can simplify equation (2) and directly solve for M_2 sin i, but this is not true for larger mass companions such as brown dwarfs and stars. We use Cox (2000) to relate host mass to spectral type. When a double-lined solution is available, the companion mass can be found from $q = M_2/M_1 = K_1/K_2$.

For all single-lined Doppler solutions, where the inclination i of a companion's orbit is unknown (no astrometric or visual solution), we assume a random distribution $P(i)$ for the orientation of the inclination with respect to our line of sight,

$$P(i)\, di = \sin(i)\, di. \tag{4}$$

From this we can find probability distributions for $\sin i$ and $\sin^3(i)$. Heacox (1995) and others suggest using either the Richardson-Lucy or Mazeh-Goldberg algorithms to approximate the inclination distribution. However, Hogeveen (1991) and Trimble (1990) argue that for small number statistics, the simple mean method produces similar results to the more complicated methods. We have large bin sizes and small number statistics, hence we use this method. The average values of the $\sin i$ and $\sin^3(i)$ distributions assuming a random inclination are $\langle \sin i \rangle = 0.785$ and $\langle \sin^3(i) \rangle = 0.589$, which are used to estimate the mass for planets and other larger single-lined spectroscopic binaries, respectively. For example, in Figure 5, of the 198 mass estimates in the 50 pc sample, 53 (27%) come from visual double-lined Doppler solutions, six (3%) come from infrared double-lined Doppler solutions (Mazeh et al. 2003), 18 (9%) come from knowing the inclination (astrometric or visual solution also available for system), 10 (5%) come from assuming that Doppler brown dwarf candidates have low inclinations, 55 (28%) come from assuming $\langle \sin i \rangle = 0.785$, and 56 (28%) from assuming $\langle \sin^3(i) \rangle = 0.589$.

REFERENCES

Armitage, P. J., & Bonnell, I. A. 2002, MNRAS, 330, L11
Barrado y Navascues, D., Stauffer, J. R., Bouvier, J., & Martin, E. L. 2001, ApJ, 546, 1006
Bate, M. R. 2000, MNRAS, 314, 33
Boss, A. P. 2002, ApJ, 576, 462
Burrows, A., et al. 1997, ApJ, 491, 856
Correia, A. C. M., Udry, S., Mayor, M., Laskar, J., Naef, D., Pepe, F., Queloz, D., & Santos, N. C. 2005, A&A, 440, 751
Cox, A. N. 2000, Allen's Astrophysical Quantities (4th ed.; New York: AIP)
Duquennoy, A., & Mayor, M. 1991, A&A, 248, 485
Els, S. G., Sterzik, M. F., Marchis, F., Pantin, E., Endl, M., & Kürster, M. 2001, A&A, 370, L1
Endl, M., Hatzes, A. P., Cochran, W. D., McArthur, B., Allende Prieto, C., Paulson, D. B., Guenther, E., & Bedalov, A. 2004, ApJ, 611, 1121
ESA. 1997, The *Hipparcos* and Tycho Catalogues (ESA SP-1200; Noordwijk: ESA), http://astro.estec.esa.nl/hipparcos
Fischer, D. A., Marcy, G. W., Butler, P. R., Vogt, S. S., & Apps, K. 1999, PASP, 111, 50
Gizis, J. E., Kirkpatrick, J. D., Burgasser, A., Reid, I. N., Monet, D. G., Liebert, J., & Wilson, J. C. 2001, ApJ, 551, L163
Gizis, J. E., Reid, I. N., Knapp, G. R., Liebert, J., Kirkpatrick, J. D., Koerner, D. W., & Burgasser, A. J. 2003, AJ, 125, 3302
Halbwachs, J. L., Arenou, F., Mayor, M., Udry, S., & Queloz, D. 2000, A&A, 355, 581
Halbwachs, J. L., Mayor, M., Udry, S., & Arenou, F. 2003, A&A, 397, 159
Hartkopf, W. I., & Mason, B. D. 2004, Sixth Catalog of Orbits of Visual Binary Stars (Washington, DC: USNO), http://ad.usno.navy.mil/wds/orb6.html
Heacox, W. D. 1995, AJ, 109, 2670
———. 1999, ApJ, 526, 928
Hillenbrand, L. A. 2004, in The Dense Interstellar Medium in Galaxies, ed. S. Pfalzner et al. (Berlin: Springer), 601
Hillenbrand, L. A., & Carpenter, J. M. 2000, ApJ, 540, 236
Hogeveen, S. J. 1991, Ph.D. thesis, Univ. Illinois, Urbana
Ida, S., & Lin, D. N. C. 2004, ApJ, 604, 388
Jiang, I.-G., Laughlin, G., & Lin, D. N. C. 2004, AJ, 127, 455
Jones, H. R. A., Butler, P. R., Marcy, G. W., Tinney, C. G., Penny, A. J., McCarthy, C., & Carter, B. D. 2002, MNRAS, 337, 1170
Konacki, M., et al. 2004, ApJ, 609, L37
Kroupa, P. 2002, Science, 295, 82
Kroupa, P., & Bouvier, J. 2003, MNRAS, 346, 369
Larson, R. B. 2003, preprint (astro-ph/0306596)
Lineweaver, C. H., & Grether, D. 2003, ApJ, 598, 1350
Lineweaver, C. H., Grether, D., & Hidas, M. 2003, in ASP Conf. Ser. 294, Scientific Frontiers in Research on Extrasolar Planets, ed. D. Deming & S. Seager (San Francisco: ASP), 161
Marcy, G. W., & Butler, P. R. 2000, PASP, 112, 137
Marcy, G. W., et al. 2001, ApJ, 555, 418
Matzner, C. D., & Levin, Y. 20045, ApJ, 628, 817
Mazeh, T., Simon, M., Prato, L., Markus, B., & Zucker, S. 2003, ApJ, 599, 1344
McCarthy, C., & Zuckerman, B. 2004, AJ, 127, 2871
Moraux, E., Bouvier, J., Stauffer, J. R., & Cuillandre, J. C. 2003, A&A, 400, 891
Nidever, D. L., Marcy, G. W., Butler, P. R., Fischer, D. A., & Vogt, S. S. 2002, ApJS, 141, 503
Pont, F., Bouchy, F., Queloz, D., Santos, N. C., Mayor, M., & Udry, S. 2004, A&A, 426, L15
Pourbaix, D., et al. 2004, A&A, 424, 727
Queloz, D., et al. 2000, A&A, 354, 99
Reid, I. N. 2002, PASP, 114, 306
Rice, W. K. M., Armitage, P. J., Bonnell, I. A., Bate, M. R., Jeffers, S. V., & Vine, S. G. 2003, MNRAS, 346, L36
Saar, S. H., Butler, P. R., & Marcy, G. W. 1998, ApJ, 498, L153
Schneider, J. 2005, Extrasolar Planets Catalog, http://www.obspm.fr/encycl/catalog.html
Slesnick, C. L., Hillenbrand, L. A., & Carpenter, J. M. 2004, ApJ, 610, 1045
Tinney, C. G., Butler, P. R., Marcy, G. W., Jones, H. R. A., Vogt, S. S., Apps, K., & Henry, G. W. 2001, ApJ, 551, 507
Trimble, V. 1990, MNRAS, 242, 79
Udry, S., Mayor, M., Naef, D., Pepe, F., Queloz, D., Santos, N. C., & Burnet, M. 2002, A&A, 390, 267
Udry, S., Mayor, M., & Santos, N. C. 2003, A&A, 407, 369
Vogt, S. S., Butler, P. R., Marcy, G. W., Fischer, D. A., Pourbaix, D., Apps, K., & Laughlin, G. 2002, ApJ, 568, 352
Wright, J. T., Marcy, G. W., Butler, P. R., & Vogt, S. S. 2004, ApJS, 152, 261
Zucker, S., & Mazeh, T. 2001a, ApJ, 562, 549
———. 2001b, ApJ, 562, 1038